

Comparing the Efficiency of Biased and Unbiased Molecular Dynamics in Reconstructing the Free Energy Landscape of Met-Enkephalin

Ludovico Sutto, Marco D’Abramo, and Francesco Luigi Gervasio*

Spanish National Cancer Research Center (CNIO), Structural Biology and Biocomputing Programme, Melchor Fernandez Almagro, 3 E-28029 Madrid, Spain

Received July 23, 2010

Abstract: All-atom unbiased molecular dynamics simulations are now able to explore the microsecond to millisecond time scale for simple biological macromolecules in an explicit solvent. This allows for a careful comparison of the efficiency and accuracy of enhanced sampling methods versus long unbiased molecular dynamics in reconstructing conformational free energy surfaces. Here, we use an equilibrium microsecond-long molecular dynamics simulation as a reference to analyze the convergence properties of well-tempered metadynamics with two different sets of collective variables. In the case of the small and very diffusive Met-enkephalin pentapeptide, we find that the performance strongly depends on the choice of the collective variables (CVs). Using a set of principal component analysis derived eigenvectors, the convergence of the FES is faster than with both hand-picked CVs and unbiased molecular dynamics.

1. Introduction

Nowadays, thanks to specialized hardware¹ and grid computing,^{2,3} it is increasingly possible to study relevant biological events including folding, molecular recognition, and conformational plasticity with long unbiased all-atom molecular dynamics (MD) simulations. Assuming ergodicity of the systems under study, these long runs can be used to calculate both kinetics and thermodynamics observables in simple systems as fast-folding proteins or small peptides. So far, due to the time-scale problem, these physical properties could only be obtained, with meaningful statistics, by enhanced sampling or coarse-grained methods.^{4–20} This is still true for more complex systems having higher free-energy barriers and characteristic times of multiple milliseconds to seconds. Enhanced sampling methods are generally based on some assumptions on the underlying system, such as the choice of meaningful collective variables or the definition of an initial and final state. Thus, a comparison of the relative performance, e.g., in terms of the convergence and accuracy of the reconstructed free energy

surfaces, obtained with the two approaches is now important and increasingly urgent.

The goal of the present paper is to compare well-tempered metadynamics,^{17,21} a widely used enhanced sampling method, with a long unbiased MD in terms of the convergence of the reconstructed free energy surface (FES). We will look at the relative computational efficiency, and at the effect of the choice and number of the collective variables (CVs) on it. In particular, we will see how a general set of collective variables automatically generated leads to a fast and accurate reconstruction of the free energy surface.

Our model system of choice is the Met-enkephalin, a pentapeptide involved in regulating nociception in the body by binding to the opioid receptors. Due to its extreme flexibility, the native structure of Met-enkephalin has been elusive experimentally.^{22,23} A variety of computational approaches have been used to explore its conformational landscape.^{24–28} Our choice was guided both by its small size and by the nature of its conformational free-energy surface. The peptide is sufficiently small to allow for an extensive unbiased all-atom explicit solvent MD simulation. Still, its free-energy surface is complex and well-structured. What is more, the small height of the free energy barriers and the

* To whom correspondence should be addressed. E-mail: flgervasio@cnio.es.

diffusive behavior of its dynamics pose an additional challenge to free-energy-based methods like well-tempered metadynamics that generally perform better in the presence of high free energy barriers and ballistic dynamics.

2. Computational Methods

The simulations were performed using version 4 of the molecular dynamics program GROMACS²⁹ with the Amber03 force field.³⁰ The Met-enkephalin, with sequence YGGFM, is solvated in 1256 tip3p water molecules³¹ enclosed in a cubic box of 38.9 nm³ under periodic boundary conditions. The van der Waals interactions were cut off at 1.4 nm, and the long-range electrostatic interactions were calculated by the particle mesh Ewald algorithm³² with a mesh spaced 0.12 nm. The neighbor list for the nonbonded interactions was updated every 0.02 ps. The system evolves in the canonical ensemble, coupled with a Nosé-Hoover thermal bath^{33,34} at $T = 300$ K and a time step of 2 fs.

The solvated system was prepared using the following steps: (1) a steepest descent energy minimization; (2) equilibration of the system for 10 ps; (3) a density equilibration with a 2 ns dynamics at 300 K and constant pressure, coupling the system to a Parrinello–Rahman barostat,³⁵ and finally (4) another 2 ns dynamics at 300 K with a Berendsen thermostat³⁶ at constant volume to thermalize the system.

We used the well-tempered variant of the metadynamics enhanced sampling technique³⁷ in which the evolving bias $V(s,t)$ at time t and CV value s is built by the sum of Gaussian-shaped potentials with decreasing height. Such an algorithm, introduced by Barducci et al.²¹ for the alanine dipeptide, has been proven more efficient than original metadynamics, guaranteeing the convergence of the free energy surface at a long time limit. According to the well-tempered metadynamics prescription, a Gaussian is deposited every 4 ps with height $W = W_0 e^{-V(s,t)/fT}$, where $W_0 = 2$ kJ/mol is the initial height, T is the temperature of the simulation, and $f = 1.5$ is the bias factor. The width of the Gaussians is set to 0.02 in units of the respective CV and determines the resolution of the recovered free energy surface.

The collective variables biasing the 250 ns dynamics performed are either one or more atomic distances (d_i) or the projection of the heavy atom positions along one or more eigenvectors (v_i). Those eigenvectors are obtained applying the essential dynamics technique,³⁸ a principal-component-based analysis (PCA), to the 40 heavy atoms of the whole unbiased trajectory leading to a 120×120 covariance matrix. This symmetric matrix represents the correlation between atomic motions in Cartesian coordinate space and the eigenvectors obtained from the diagonalization of the collective motions. The eigenvectors corresponding to the largest eigenvalues contain the largest fluctuations and hence hold the most important motions of the system. The four largest eigenvalues of the covariance matrix describe 32.0%, 13.6%, 12.3%, and 10.0% of the fluctuations.

The same analysis repeated using only the first 210 ns or 21 ns (10% and 1% of the simulation time, respectively) of the unbiased trajectory showed similar results. In particular, the overlap between the subspace generated by the first two

eigenvectors calculated after the first 21 ns and the reference subspace generated by the first two eigenvectors of the whole 2.1 μ s trajectory is 0.72, where 1 is a complete overlap. The overlap increases up to 0.94 using the eigenvectors obtained after 210 ns. The overlap is calculated as the root-mean-square inner product of the first two PCA eigenvectors.³⁹

To perform the metadynamics run, we modified the PLUMED⁴⁰ plug-in for GROMACS, introducing the eigenvectors as new collective variables. The reweighting procedure described by Bonomi et al.⁴¹ was used to calculate the projection of the FES on other CVs than the ones used to bias the dynamics.

To quantitatively compare a metadynamics reconstructed FES $F_i(s)$ to the reference unbiased molecular dynamics FES $F_{\text{ref}}(s)$ expressed in terms of the CVs defined in a region Ω , we used two different parameters: (i) The distance measure introduced by Alonso and Echenique is used:⁴² $d_A(F_i, F_{\text{ref}}) = [(\sigma_i^2 + \sigma_{\text{ref}}^2)(1 - r_{i,\text{ref}}^2)]^{1/2}$ where σ_x , with x denoting either i or ref, is the statistical variance of the free energy F_x defined by $\sigma_x = 1/N \int_{\Omega} (F_x(s) - \langle F_x \rangle)^2 ds$ where $\langle F_x \rangle = 1/N \int_{\Omega} F_x(s) ds$ is the average value of F_x in the region Ω and $N = \int_{\Omega} ds$ is the normalization. The variances σ_x set the physical scale of the measure and confer the energy units to the distance. $r_{i,\text{ref}}$ is the Pearson correlation coefficient and measures the degree of correlation between the two energy surfaces. It is defined by $r_{i,\text{ref}} = \text{cov}(F_i, F_{\text{ref}}) / (\sigma_i \sigma_{\text{ref}})$ where $\text{cov}(F_i, F_{\text{ref}})$ is the covariance between the two free energies. Globally, the d_A measure is convenient since it is expressed in energy units and can be directly compared to the thermal fluctuations. (ii) The Kullback–Leibler divergence is used:⁴³ $\text{KLDiv}(F_i, F_{\text{ref}}) = \int_{\Omega} \exp(-F_{\text{ref}}(s)/k_B T) (F_i(s) - F_{\text{ref}}(s)) / k_B T ds$ expressed in terms of the free energies rather than the probabilities P_i , making use of the relation $F_i = -k_B T \ln(P_i)$, where k_B is Boltzmann's constant and T is the temperature. It should be noted that it is dimensionless and not symmetric. Such a parameter gives an interesting and slightly different measure of the FES similarity, weighting the relevant regions more, i.e., the free energy minima and valleys of the reference surface, as compared to the high free energy ones.

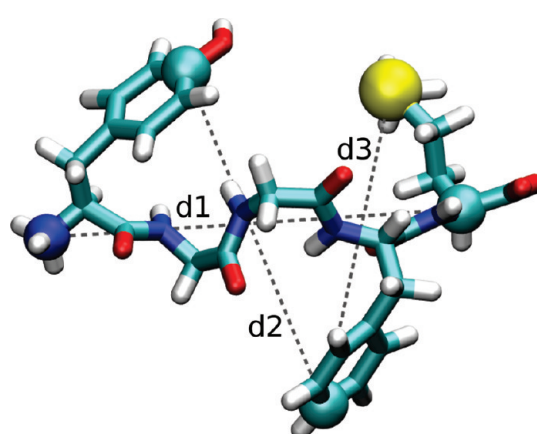


Figure 1. Met-enkephalin with the three distances used as structural observables: $d_1 = \text{dist}(\text{TYR1:N}, \text{MET5:CA})$, $d_2 = \text{dist}(\text{TYR1:CZ}, \text{PHE4:CZ})$, $d_3 = \text{dist}(\text{MET5:SD}, \text{PHE4:CZ})$.

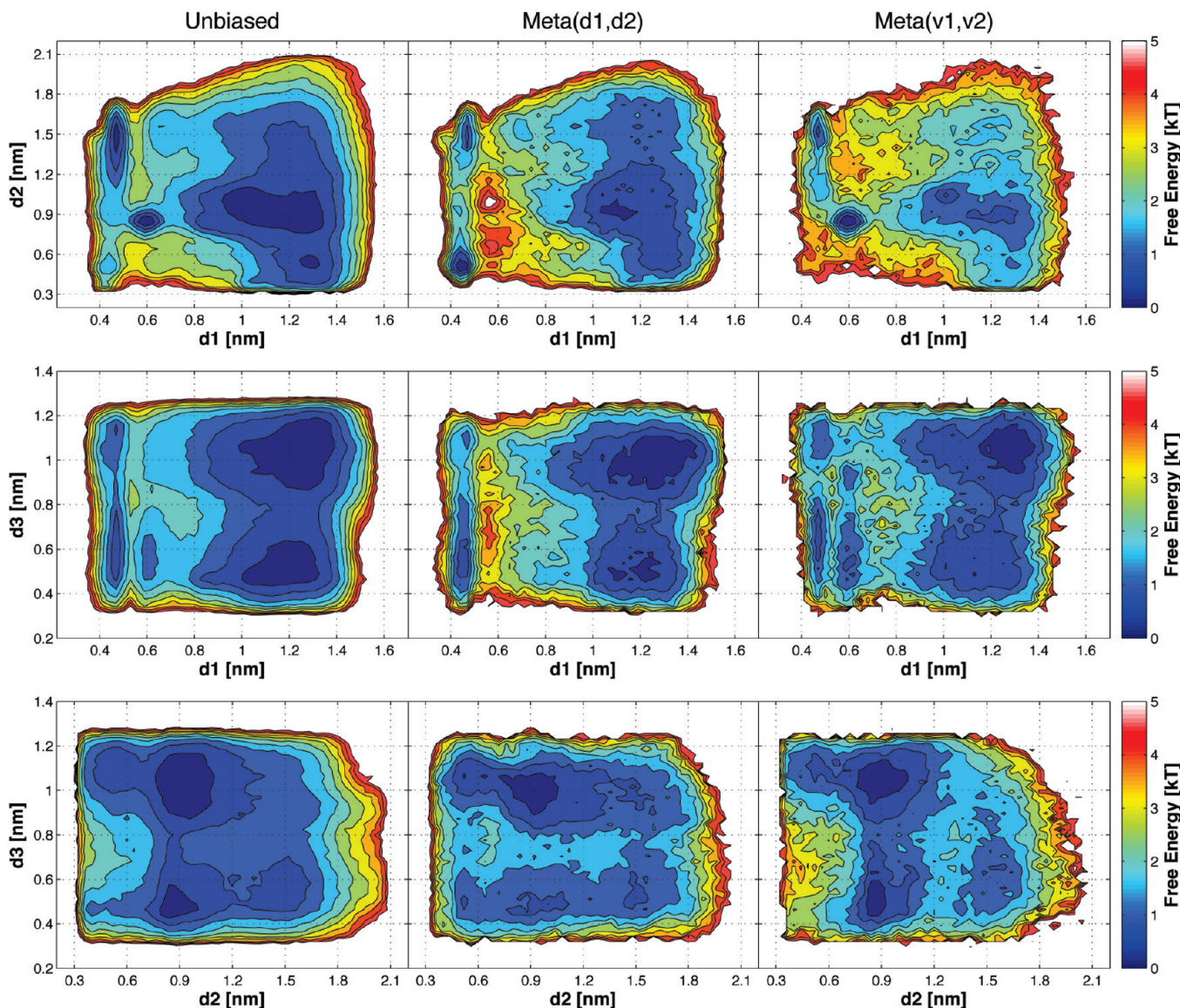


Figure 2. Free energy surfaces as a function of the distances d_1 , d_2 , and d_3 for the reference unbiased simulation and two metadynamics simulations using respectively (d_1, d_2) and (v_1, v_2) as biases. The contour lines are drawn every $0.5 k_B T$.

3. Results and Discussion

The reference FES is obtained from a $2.1 \mu s$ unbiased simulation, whose convergence with respect to the FES was checked by block analysis (see Supporting Information). The metadynamics runs are performed using two different sets of collective variables, namely, the distances between atoms shown in Figure 1 and the projections along the first PCA eigenvectors (see Computational Methods). The former CVs have been chosen to intuitively describe the conformational space of the peptide backbone and side chains. Such a set was extracted from a visual inspection of the structures sampled in the unbiased trajectory. The latter CVs take advantage of the essential dynamics technique^{38,44} and have been shown to be much more efficient than standard clustering in reducing data and reproducing salient features of protein folding.⁴⁵ They have also been used to compress MD trajectories⁴⁶ and, with standard metadynamics, to explore the free energy landscape of dialanine and SH3 domain.⁴⁷

The two-dimensional FESs obtained as a function of (d_1, d_2) , (d_1, d_3) , and (d_2, d_3) are shown in Figure 2. The unbiased $2.1 \mu s$ reference simulation (Figure 2, first column) presents barriers smaller than $2 k_B T$ as expected for a diffusive system.

The same free energy projections are overall well reconstructed already after 100 ns in the two 2-CVs metadynamics runs (Figure 2, center and right columns). Nevertheless, some discrepancies emerge in a more detailed comparison. In particular, the reconstructed landscape in the case of the distance metadynamics (Figure 2, center column, first row) completely misses the minimum at $(d_1, d_2) = (0.6, 0.9)$, showing in its place a high barrier. On the contrary, the eigenvector metadynamics (Figure 2, right column) recovers within $0.5 k_B T$ all four minima, and the overall pattern of the valleys similarly agrees. This holds also for $\text{FES}(d_1, d_3)$ and $\text{FES}(d_2, d_3)$, in which the eigenvector metadynamics performs better than the metadynamics using d_1 and d_2 as CVs. In the case of the metadynamics using d_1 , d_2 , and d_3 as CVs, 100 ns is not enough to correctly reproduce the free

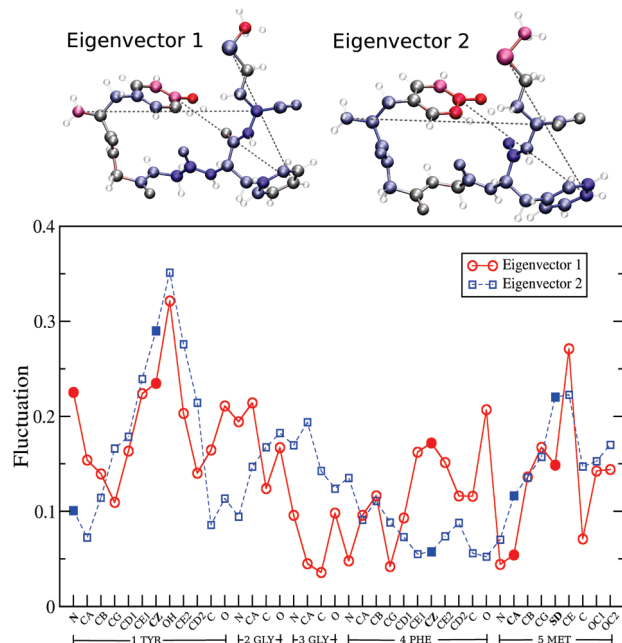


Figure 3. The 40 components of the first two PCA eigenvectors v_1 and v_2 . Two identical balls-and-sticks Met-enkephalin conformations are drawn with the 40 heavy atoms colored by their average fluctuation on a scale from highest value (red) to lowest (blue) for both of the two principal eigenvectors. The distances d_1 , d_2 , and d_3 are depicted as dashed lines between the atoms. In the graph, the same information is represented quantitatively. The five filled symbols represent the atoms involved in either the d_1 , d_2 , or d_3 distance definition.

energies $\text{FES}(d_1, d_3)$ and $\text{FES}(d_2, d_3)$ (see the Supporting Information), while the simulation with v_1 , v_2 , and v_3 performs as well as the metadynamics with v_1 and v_2 (see the Supporting Information and Figure 2).

The reason underlying the worse performance of hand-picked distance CVs over the projection over the principal components can be better understood checking the fluctuation content of each atom. In Figure 3 are shown the components of the first two eigenvectors v_1 and v_2 for each one of the 40 heavy atoms. The five atoms involved in the three chosen distances link highly fluctuating regions even though they are not the most fluctuating ones. Clearly, any set of a few atoms cannot fully describe the conformational motions since their distances only take into account a limited number of degrees of freedom. This suggests that the choice of the eigenvectors as natural CVs has two main advantages. First, the eigenvectors intrinsically describe the largest conformational changes and can be easily obtained from a preliminary unbiased simulation. Second, such a choice avoids the frustrating task of the quest of the most efficient CVs.

Hence, in the cases where the interest is to focus on slow collective motions, like in protein conformational changes, or where the choice of the CV is not trivial, the use of eigenvectors provides both a simple and physically meaningful alternative. It is worth it to mention that the set of PCA eigenvectors always represents a complete and orthogonal basis, avoiding *a priori* a linear correlation among CVs which would lead to inefficient sampling. The number of eigenvectors used as CVs can be increased at will, eventually reaching a complete representation of the degrees of freedom

of the system. This is mathematically exact when the number of eigenvectors equals the number of degrees of freedom. However, in practice, a very accurate representation can be reached with a much smaller number of eigenvectors, permitting a dramatic reduction in the size of the CV space.^{45,46}

The ability of these “natural” CVs to exhaustively explore the conformational space is also reflected by the accuracy of the reconstructed FES projected along two different and global observables as the root-mean-square deviation from a reference structure (rmsd) and the radius of gyration (rgyr) shown in Figure 4. In fact, the position of the minimum and the overall topology of the free energy landscape of the metadynamics run completely agree with the reference unbiased simulation. Moreover, if we compare the time convergence of the metadynamics FES to the reference FES with respect to the unbiased MD, we observe how these CVs allow the system to explore larger regions of conformational space in less time. In fact, although a fair convergence is achieved within 100 ns with all of the tested CVs (distances and eigenvectors), the eigenvector metadynamics provides a FES that closely resembles the reference FES as early as after 50 ns (see Figure 4). On the other hand, unbiased simulation after neither 50 nor 100 ns explored the region at $(\text{rmsd}, \text{rgyr}) \approx (0.31, 0.40-0.43)$.

To compare our sampled conformations to the literature values, we extracted the representative geometries for each of the three shallow minima present in the $\text{FES}(v_1, v_2)$ shown in Figure 5. Even though we used different observables than Sanbonmatsu and García,²⁷ since their PCA eigenvectors were obtained only from the five C-alpha motions, some common features are apparent. In particular, the minimum (A) corresponds to the same U-shaped conformation found by Sanbonmatsu and García²⁷ and by Henin et al.,²⁸ in which the phenylalanine and tyrosine side chains are packed. In the other two minima, the backbone is more elongated, and the system explores both extended (B) and helix-like (C) conformations, also in agreement with the aforementioned works. Interestingly, these minima are connected in the essential space, indicating the absence of relevant barriers in agreement with the high flexibility of this peptide.

Finally, in order to assess the convergence of the free energy as a function of the number of collective variables, we used two different parameters: (i) the correlation coefficient introduced by Alonso and Echenique,⁴² which allows quantitative measurement of the similarity between different energy potentials, and (ii) the Kullback–Leibler divergence,⁴³ which weights the free energy minima more with respect to poorly sampled regions (see Computational Methods). These two coefficients are used as different measures of the distance between the reconstructed FES provided by the metadynamics runs and the reference $\text{FES}(\text{rmsd}, \text{rgyr})$ of the unbiased MD simulation.

In Figure 6, we report these coefficients for both the eigenvector metadynamics and distance metadynamics compared to the unbiased MD run as a function of time. Both coefficients and both sets of CVs give a similar result and show that the metadynamics runs converge faster than the unbiased run. The metadynamics with two and three

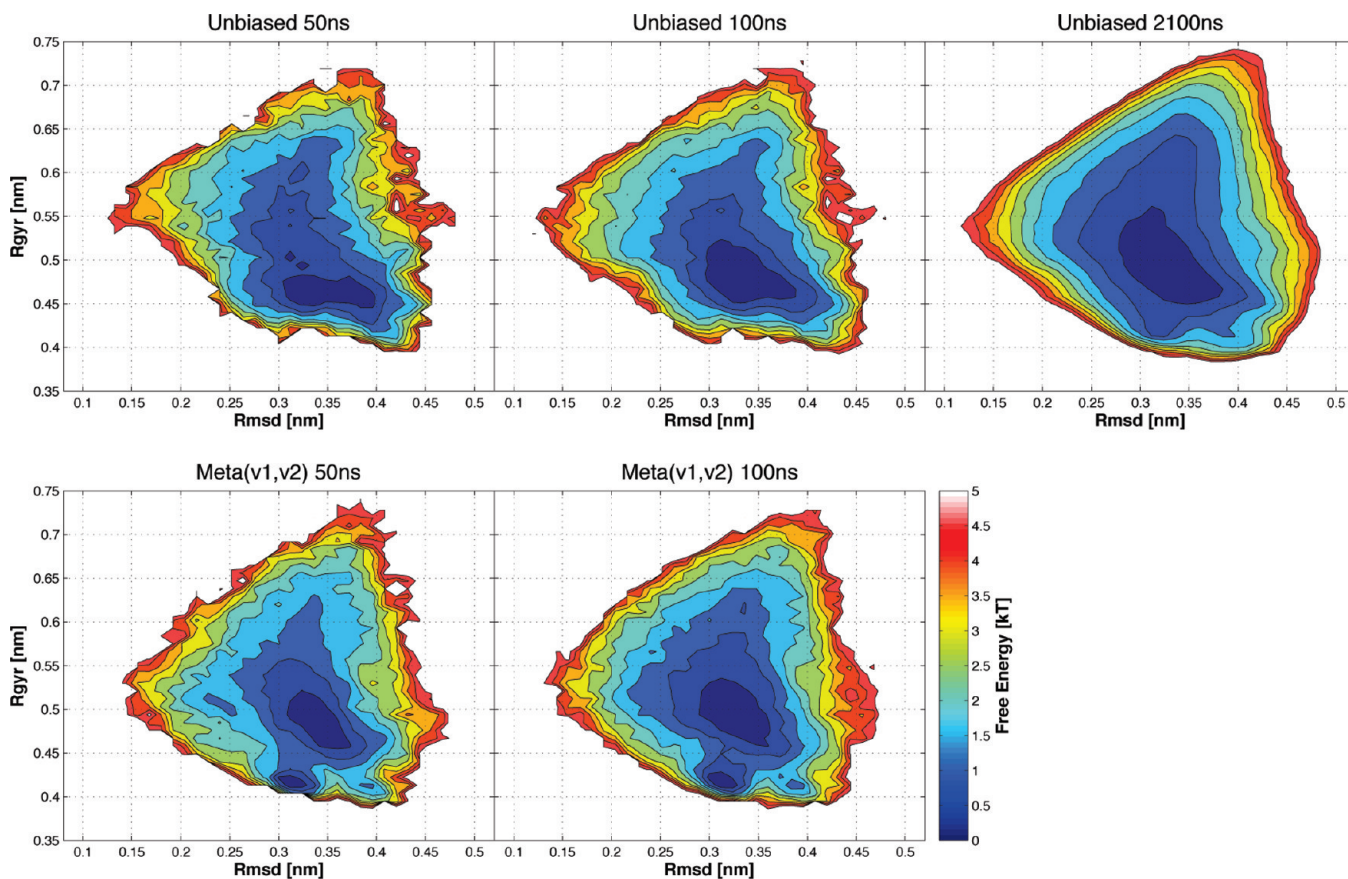


Figure 4. Free energy surfaces for different times as a function of the root-mean-square deviation (rmsd) and the gyration radius (rgyr) for the reference unbiased simulation and the metadynamics simulation using (v_1, v_2) as a bias. The contour lines are drawn every $0.5 k_B T$.

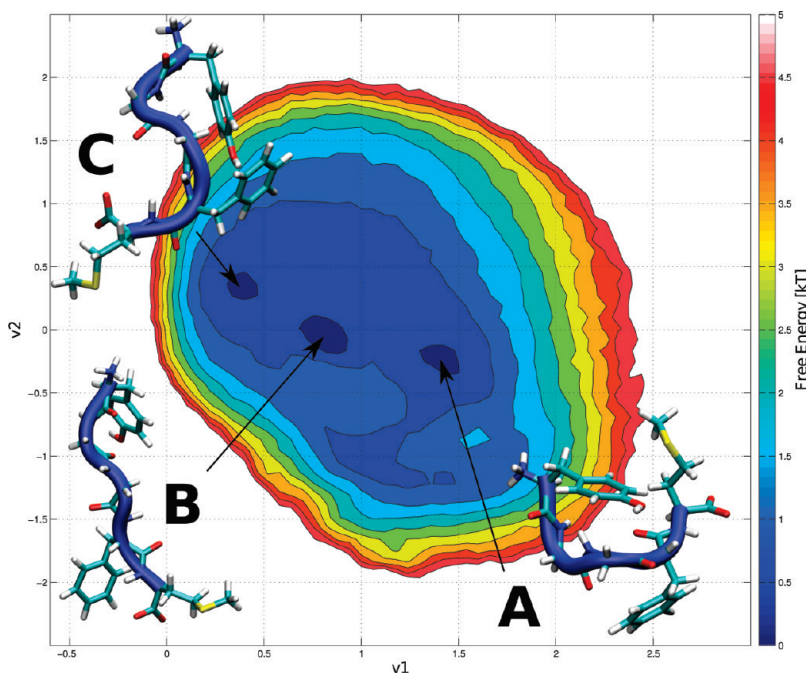


Figure 5. Free energy surface as a function of the projection over the two principal eigenvectors v_1 and v_2 with contour lines every $0.5 k_B T$. The representative conformations of the three minima are also shown as insets and correspond to (A) a U-shaped backbone with packed aromatic rings, (B) an elongated conformation, and (C) a helix-like structure.

eigenvectors reach, and stay, below a $1 k_B T$ reference threshold before any other run. As for the convergence as a function of the number of CVs, we expect that less

vectors (or distances) can miss important degrees of freedom, while too many CVs slow down the metadynamics filling time. This is reflected in the longer time

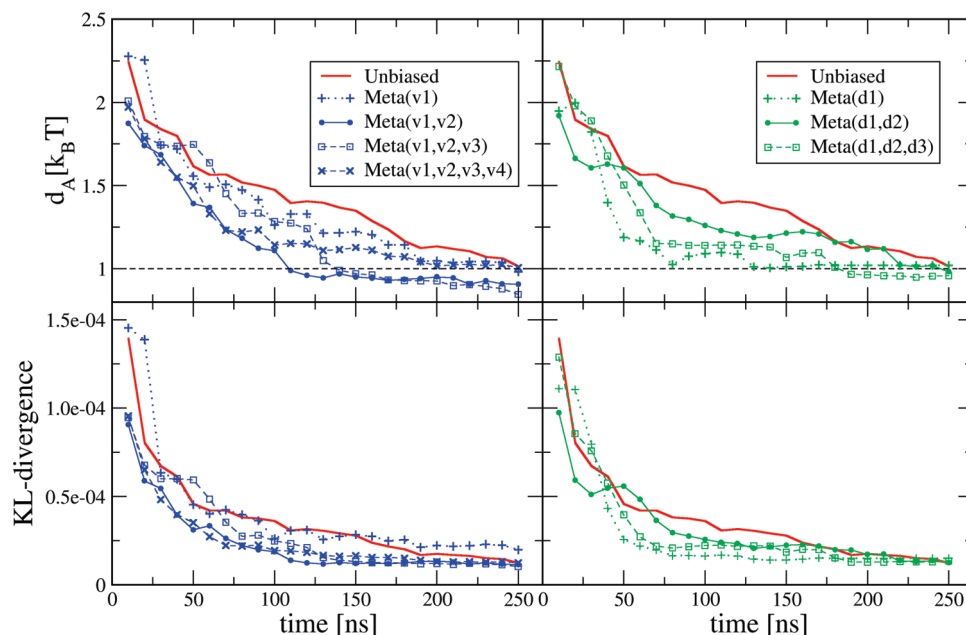


Figure 6. Comparison of the convergence of the free energy two-dimensional surface FES(rmsd,rgyr) for the eigenvector (blue, left-hand-side panels) and distance (green, right-hand-side panels) metadynamics simulations as a function of time. In red is shown the unbiased simulation. The similarities are calculated using as reference the $2.1\ \mu\text{s}$ unbiased simulation FES shown in Figure 4. In the upper panels, the metric d_A is the energy-function distance introduced by Alonso and Echenique⁴² and has units of $k_B T$. A dashed line at $1\ k_B T$ defines the goal accuracy. In the lower panels, the similarity is computed using the Kullback–Leibler divergence.⁴³

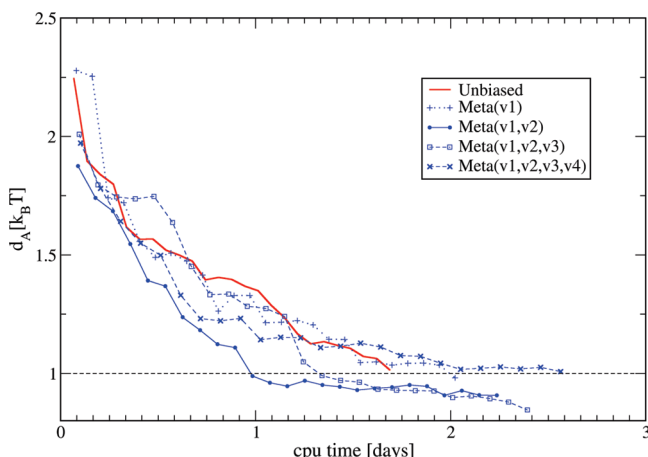


Figure 7. Comparison of the computer simulation time as a function of the distance d_A of the reconstructed FES(rmsd,rgyr) to the reference one, for the unbiased (red) and the eigenvector metadynamics simulations (blue). The computer time refers to a run that uses 24 CPUs on a parallel cluster. The points are plotted every 10 ns of simulation, for a total of 250 ns, time at which all of the simulations have reached the $1\ k_B T$ accuracy threshold represented by the dashed line.

needed by the metadynamics with one and four eigenvectors to reach the goal accuracy.

Clearly, two PCA vectors strike the right balance and converge the fastest, as seen in Figure 7, where we show the accuracy, in terms of the distance d_A to the reference FES, as a function of the actual computer time needed to reach it. After 110 ns, the equivalent of about one day of 24 parallel CPU usage, the metadynamics with v_1 and v_2 reconstructs the FES(rmsd,rgyr) with an accuracy below the $1\ k_B T$ threshold. The same accuracy is reached after 140 ns,

or 32 CPU h for the metadynamics with three eigenvectors. The metadynamics with only v_1 and with the four eigenvectors eventually reach the goal after 250 ns, performing worse than the unbiased run.

4. Conclusions

In this paper, we compared the accuracy and computational efficiency of long unbiased MD simulations and well-tempered metadynamics in reconstructing the conformational free energy landscape of a peptide. Given the nature of the test case shown, which has low free energy barriers and diffusive dynamics, the advantage of free energy methods with respect to unbiased MD should be greatly reduced. Nevertheless, we found that, with a rationally built set of collective variables, well-tempered metadynamics is able to reconstruct an accurate free energy surface quicker than unbiased MD. These CVs, i.e., the eigenvectors describing the principal directions of motion, constitute a natural set which can be easily obtained from a preliminary unbiased MD simulation. On the contrary, simple, yet hand-picked, collective variables, as a set of chosen distances, turn out to miss some relevant features of the free energy surface. These results confirm the importance of the choice of the CVs but also provide a simple approach to automatically define a set of CVs that can be applied to reconstruct the FES of more complex systems, where higher free energy barriers make the convergence of unbiased MD simulation problematic.

Acknowledgment. The authors acknowledge S. Piana for useful discussions and advice and the Barcelona Supercomputing Center for a generous allocation of computer resources.

Supporting Information Available: Figures of free energy surface, a table presenting block analysis of the distance d_A and KL-divergence calculated for the unbiased trajectory, and a figure presenting a comparison of the convergence of the free energy two-dimensional surface FES(rmsd,rgyr) for the eigenvector and distance metadynamics simulations as a function of time. This material is available free of charge via the Internet at <http://pubs.acs.org>.

References

- (1) Klepeis, J. L.; Lindorff-Larsen, K.; Dror, R. O.; Shaw, D. E. *Curr. Opin. Struct. Biol.* **2009**, *19*, 120–127.
- (2) Shirts, M.; Pande, V. S. *Science* **2000**, *290*, 1903–1904.
- (3) Buch, I.; Harvey, M. J.; Giorgino, T.; Anderson, D. P.; Fabritiis, G. D. *J. Chem. Inf. Model.* **2010**, *50*, 397–403.
- (4) Patey, G. N.; Valleau, J. P. *J. Chem. Phys.* **1975**, *63*, 2334–2339.
- (5) Grubmüller, H. *Phys. Rev. E* **1995**, *52*, 2893–2906.
- (6) Kumar, S.; Rosenberg, J. M.; Bouzida, D.; Swendsen, R. H.; Kollman, P. A. *J. Comput. Chem.* **1995**, *16*, 1339–1350.
- (7) Jarzynski, C. *Phys. Rev. Lett.* **1997**, *78*, 2690.
- (8) Darve, E.; Pohorille, A. *J. Chem. Phys.* **2001**, *115*, 9169–9183.
- (9) Gullingsrud, J.; Braun, R.; Schulten, K. *J. Comput. Phys.* **1999**, *151*, 190–211.
- (10) Rosso, L.; Minary, P.; Zhu, Z. W.; Tuckerman, M. E. *J. Chem. Phys.* **2002**, *116*, 4389–4402.
- (11) Elber, R.; Karplus, M. *Chem. Phys. Lett.* **1987**, *139*, 375–380.
- (12) Maragliano, L.; Fischer, A.; Vanden-Eijnden, E.; Ciccotti, G. *J. Chem. Phys.* **2006**, *125*, 024106.
- (13) Dellago, C.; Bolhuis, P.; Csajka, F. S.; Chandler, D. *J. Chem. Phys.* **1998**, *108*, 1964–1977.
- (14) Juraszek, J.; Bolhuis, P. G. *Proc. Natl. Acad. Sci. U.S.A.* **2006**, *103*, 15859–15864.
- (15) Merlitz, H.; Wenzel, W. *Chem. Phys. Lett.* **2002**, *362*, 271–277.
- (16) Sugita, Y.; Okamoto, Y. *Chem. Phys. Lett.* **1999**, *314*, 141–151.
- (17) Laio, A.; Gervasio, F. L. *Rep. Prog. Phys.* **2008**, *71*, 126601.
- (18) Bussi, G.; Gervasio, F. L.; Laio, A.; Parrinello, M. *J. Am. Chem. Soc.* **2006**, *128*, 13435–13441.
- (19) Camilloni, C.; Sutto, L. *J. Chem. Phys.* **2009**, *131*, 245105.
- (20) Tozzini, V. *Curr. Opin. Struct. Biol.* **2005**, *15*, 144–50.
- (21) Barducci, A.; Bussi, G.; Parrinello, M. *Phys. Rev. Lett.* **2008**, *100*, 020603.
- (22) Graham, W. H.; Carter, E. S. I.; Hicks, R. P. *Biopolymers* **1992**, *1755*–1764.
- (23) D'Alagni, M.; Delfini, M.; Di Nola, A.; Eisenberg, M.; Paci, M.; Roda, L. G.; Veglia, G. *Eur. J. Biochem.* **1996**, *240*, 540–549.
- (24) Shen, M.; Freed, K. *Biophys. J.* **2002**, *82*, 1791–1808.
- (25) Bartels, C.; Karplus, M. *J. Phys. Chem. B* **1998**, *102*, 865–880.
- (26) Li, Z. Q.; Scheraga, H. A. *Proc. Natl. Acad. Sci. U.S.A.* **1987**, *84*, 6611–6615.
- (27) Sanbonmatsu, K. Y.; García, A. E. *Proteins* **2002**, *46*, 225–34.
- (28) Henin, J.; Fiorin, G.; Chipot, C.; Klein, M. L. *J. Chem. Theory Comput.* **2010**, *6*, 35–47.
- (29) Hess, B.; Kutzner, C.; van der Spoel, D.; Lindahl, E. *J. Chem. Theory Comput.* **2008**, *4*, 435–447.
- (30) Duan, Y.; Wu, C.; Chowdhury, S.; Lee, M. C.; Xiong, G.; Zhang, W.; Yang, R.; Cieplak, P.; Luo, R.; Lee, T.; Caldwell, J.; Wang, J.; Kollman, P. *J. Comput. Chem.* **2003**, *24*, 1999–2012.
- (31) Mahoney, M. W.; Jorgensen, W. L. *J. Chem. Phys.* **2000**, *112*, 8910–8922.
- (32) Essman, U.; Perela, L.; Berkowitz, M. L.; Darden, T.; Lee, H.; Pedersen, L. G. *J. Chem. Phys.* **1995**, *103*, 8577–8592.
- (33) Nosé, S. *Mol. Phys.* **1984**, *52*, 255–268.
- (34) Hoover, W. G. *Phys. Rev. A* **1985**, *31*, 1695–1697.
- (35) Parrinello, M.; Rahman, A. *J. Appl. Phys.* **1981**, *52*, 7182–7190.
- (36) Berendsen, H. J. C.; Postma, J. P. M.; Di Nola, A.; Haak, J. R. *J. Chem. Phys.* **1984**, *81*, 3684–3690.
- (37) Laio, A.; Parrinello, M. *Proc. Natl. Acad. Sci. U.S.A.* **2002**, *99*, 12562.
- (38) Amadei, A.; Linssen, A. B. M.; Berendsen, H. J. C. *Proteins: Struct. Funct. Genet.* **1993**, *17*, 412–425.
- (39) Amadei, A.; Ceruso, A.; Di Nola, A. M. *Proteins: Struct. Funct. Genet.* **1999**, *36*, 419–424.
- (40) Bonomi, M.; Branduardi, D.; Bussi, G.; Camilloni, C.; Provasi, D.; Raiteri, P.; Donadio, D.; Marinelli, F.; Pietrucci, F.; Broglia, R. A. *Comput. Phys. Commun.* **2009**, *180*, 1961–1972.
- (41) Bonomi, M.; Barducci, A.; Parrinello, M. *J. Comput. Chem.* **2009**, *1615*–1621.
- (42) Alonso, J. L.; Echenique, P. A. *J. Comput. Chem.* **2006**, *27*, 238–252.
- (43) Kullback, S.; Leibler, R. *Ann. Math. Stat.* **1951**, *22*, 79–86.
- (44) Amadei, A.; Linssen, A. B. M.; de Groot, B. L.; van Aalten, D. M. F.; Berendsen, H. J. C. *J. Biomol. Struct. Dyn.* **1996**, *13*, 615–625.
- (45) Rajan, A.; Freddolino, P. L.; Schulten, K. *Plos One* **2010**, *5*, e9890.
- (46) Meyer, T.; Ferrer-Costa, C.; Perez, A.; Rueda, M.; Bidon-Chanal, A.; Luque, F.; Laughton, C.; Orozco, M. *J. Chem. Theory Comput.* **2006**, *2*, 251–258.
- (47) Spiwok, V.; Lipovová, P.; Králová, B. *J. Phys. Chem. B* **2007**, *111*, 3073–3076.

CT100413B